Short title [Lignin signature in humic acids, index for soil carbon stabilization]

Pyrolytic appraisal of the lignin signature in soil humic acids: assessment of its usefulness as carbon sequestration marker

I. Miralles[a], A. Piedra-Buena[b], G. Almendros[b], F.J. González-Vila[c], J.A. González-Pérez[c]*

[a] *Departamento de Desertificación y Geoecología, EEZA-CSIC, La Cañada de San Urbano, E-04230 Almería, Spain,* [b] *Museo Nacional de Ciencias Naturales, MNCN-CSIC, Serrano 115B, E-28006 Madrid, Spain,* [c] *Instituto de Recursos Naturales y Agrobiología de Sevilla, IRNAS-CSIC, Avda. Reina Mercedes, 10, E-41012 Seville, Spain.*

*) Corresponding author: J.A. González-Pérez E-mail: jag@irnase.csic.es

Abstract

Lignin markers in humic acids (HA, the alkali-soluble, acid-insoluble soil organic matter fraction) molecular features are explored to assess the extent to which plant biomacromolecules are progressively transformed by humification processes leading to stable C-forms in soils. Humic acids extracted from a collection of mountain calcimorphic soils from Sierra María-Los Vélez Natural Park (Southeastern Spain) under different use and management practices were studied in detail by visible and infrared (FT-IR) spectroscopies and analytical pyrolysis (Py-GC/MS). The HAs display a more or less marked lignin pattern defined by characteristic methoxyphenol assemblages released after pyrolysis that are associated to a typical infrared pattern including absorption frequencies bands at 1510, 1460,

1420, 1270, 1230 and 1030 cm^{-1}. This variability in the HA spectroscopic and pyrolytic patterns was used as a source of molecular-level surrogates to establish the balance between complementary mechanisms of soil C sequestration *i.e.*, a selective preservation of lignin associated to raw organic matter and other plant-inherited macromolecules, or alternative mechanisms involving microbial breakdown or plant precursors and its condensation with microbial metabolites.

We found that HAs in which the lignin signature was comparatively less marked also show high optical density values suggesting unsubstituted, condensed aromatic units and a chaotic organic structure, pointing to the presence of highly resilient carbon forms. Upon analytical pyrolysis, one group of HAs produced major yields of methoxyl-lacking aromatics (alkylbenzenes and alkylphenols), and poor yields of alkyl compounds, which suggest efficient cleavage of biomacromolecules and the occurrence of active microbial synthesis and condensation processes. In fact, these HAs also displayed broadband IR spectra, and visible spectra showing high optical density and polynuclear quinoid chromophors considered of fungal origin. Other group of HAs yielded upon pyrolysis conspicuous series of methoxyphenols and well-defined alkyl series (alkanes, alkenes and fatty acids). The IR spectra also displayed clear lignin and amide bands, as well as intense 2920 cm^{-1} band and a low optical density, indicative of a marked aliphatic character. This latter is interpreted as the result of recent diagenetic alteration processes of young organic matter and suggests that C sequestration mechanisms in these soils are mainly based on the stabilization of HAs from plant biomacromolecules and aliphatic structures.

These differential lignin alteration patterns indicate that HAs are responsive to soil C sequestration mechanisms, which in the studied soils seem to relay upon microtopographical features rather than to changes in soil use and management.

Keywords: Lignin; humic acids; humification mechanisms; calcimorphic soils.

1. Introduction

Despite the crucial global implications of carbon (C) stored in soils and sediments [1], the biogeochemical processes involved in C stabilization are not well understood [2]. The study of the molecular structure and variability in soil organic matter (SOM) may help in unravelling such stabilization processes as well as to infer resilience characteristics of different SOM fractions [3, 4]. Although humification is an active process involving biological cleavage of plant and microbial biomass followed by secondary condensation of soluble products into humic substances [5], in some circumstances biodegradation is severely hampered by climatic, biotic or mineralogical soil-forming factors leading to accumulation of raw humus types [6]. In these cases the composition of the resulting humic substances could be described as a dynamic heterogeneous mixture of relatively low molecular size components associated via hydrophobic interactions and hydrogen bonds [7]. While at the early humification stages such a supramolecular conformation could be stabilized mainly by weak dispersive forces instead of covalent linkages [8], defining a conceptual model which accounts for their essential role in providing and maintaining soil physical and chemical quality [9], at advanced humification—maturation—stages the humic substances show an outstanding intrinsic resilience and this is crucial to define soil biogeochemical quality of soils temporarily behaving as active C sinks. In particular progressive organo-metallic interactions and additional free-radical condensation of the three-dimensionally bridged structure of humic substances in the course of progressive transformation—maturation—stages may end in comparatively rigid condensed domains. In this situation most of the humic structure could consists of a 'megamolecule' formed by a network of C–C and C–O links, where discrete structural units can no longer be recognizable due to the similar stability to chemical and biological degradation of all bonds involved in the whole structure [3]. Such

SOM advanced transformation stage is often found in continental Mediterranean semiarid environments where abiotic factors *i.e.* contrasting temperature and moisture levels, sunlight exposure and the historical effect of wildfires, may lead to soils with low SOM content but highly stable and resistant to biodegradation (resilient).

In this line, several studies have pointed out the possibility to use the structural information provided by the molecular characterization of SOM to differentiate between a) ecosystems where soil C sequestration relies upon microbial mediated processes with an intense reworking and abiotic condensation of precursors producing intrinsically resilient macromolecular humic substances of chaotic structure and b) soils where the preservation of raw organic matter prevails and depends on extrinsic factors—mainly organo-mineral interactions—leading to a organic matter organization that is accessible to soil enzymes [10]. Adopting extreme positions about soil C sequestration mechanisms debate have frequently led to hermeneutic controversies in the search of a unified theory justifying SOM stabilization [11]. In particular, calcimorphic soils could be especially suitable to analyze qualitative and quantitative features relevant in the dynamics of SOM. This is due to the fact that these soils displays peculiar features associated both with e.g. microencapsulation processes of particulate plant-inherited materials [12, 13] but also with active insolubilization mechanisms of the mineral matrix related to the release of low molecular weight compounds onto a Ca^{2+} saturated soil solution [14]. In fact, the prevailing limestone substrate in semiarid Southern Spain's soils has been considered to play a role in the low structural variability in the molecular structure of the HAs [12]. This situation demands the use of accurate analytical techniques (*i.e.,* analytical pyrolysis) betraying environmental proxies (molecular markers) responsive of the different sources of environmental variability reflected in the composition of the SOM [15–17].

In the present study analytical pyrolysis (Py-GC/MS) together with visible and IR spectroscopies, are used to study HAs molecular structure and to find compositional descriptors informative about C stabilization processes in a variety of semiarid ecosystems developed on calcimorphic soils.

2. Material and methods

2.1. Soil sampling

The area of study is located in the Natural Park Sierra María-Los Vélez (Almería, Southeastern Spain) which includes a wide variety of semiarid ecosystems both seminatural (forests and brushwood) and disturbed (almond-tree orchards and cereal fields) developed on calcimorphic soils. The natural vegetation consists of pine forests (> 90 yr), oak forests, reforested pine forests, brushlands, almond-tree orchards and cereal crops (Table 1) [18]. The climate is Mediterranean-type, with typical continental features ranging from semiarid to subhumid. Temperatures are 11.9–16.9 °C with a dry summer season; rainfall events are intense and occasional. The geological substrate consists of sedimentary rocks (limestones, marls and dolomites) and soils are Rendzic and Lithic Leptosols, Calcic, Petrocalcic and Hypercalcic Chernozems, Kastanozems and Hypercalcic, Luvic and Petrocalcic Calcisols [19].

Soil samples (*ca.* 500 g) were collected with a spade from the uppermost horizon (0–10 cm) after litter removal. In the laboratory, composite samples (obtained by mixing three subsamples taken *c.* 20 m apart in the field) were air-dried and sieved to fine earth (< 2 mm) before analysis.

2.1. Physical and-chemical analyses

Soil pH was measured in a 1:1 soil:water suspension. Total carbonates were measured as $CaCO_3$ with the Bernard calcimeter [20]. The soil water holding capacity was estimated at -1.5 and -0.33 MPa in a pressure-membrane extractor [21]. Total nitrogen was determined by micro-Kjeldahl digestion and soil C by wet oxidation using dichromate in acid medium followed by redox titration [22]. Cation exchange capacity (CEC) and exchangeable ions Ca^{2+}, Mg^{2+}, K^{+}, and Na^{+} were measured after extraction with ammonium acetate solutions (1 mol L^{-1} NH_4Ac at pH 7) [23].

2.2. Soil organic matter fractionation

The methods applied for the isolation and quantitative determination of the humus fractions were based on standard procedures [14, 24]. The separation of the particulate, low density fraction (floating organic particles not yet transformed into humic substances, which in some cases may include some charcoal) was carried out by flotation using soil samples of 10 g suspended in 2 mol L^{-1} H_3PO_4. After rotary stirring for 1 min, the floating soil fraction or free organic matter was isolated by centrifuging the suspension and filtering, washed with distilled water and analyzed for total C. The soil pellet remaining after centrifugation was resuspended in 0.1 mol L^{-1} $Na_4P_2O_7$ (horizontal motion mechanical shaking for 3 h) and centrifuged. This treatment was repeated up to 3 times followed by 2 additional extractions with 0.1 mol L^{-1} NaOH; the dark brown extracts successively obtained (corresponding to the total humic extract: HA + fulvic acid) were aggregated. Two aliquots were taken from this extract, and precipitated with H_2SO_4 (1:1 by vol.) for further determination of the amounts of the acid-soluble fulvic acid and the precipitated HA fraction. The soil residue after the alkaline extraction was washed with distilled water and desiccated at 40 °C. The C concentration in this residue corresponded to the total humin.

147 *2.3. Preparative isolation and purification of the HA fraction*

148 Qualitative isolation and purification (de-ashing) of the HAs was performed by precipitating
149 the total humic extract with 6 mol L^{-1} HCl to pH= 2, centrifuging, redissolving the acid
150 insoluble HA in 0.5 mol L^{-1} NaOH and high-speed centrifuging at 43500 *g*. The
151 centrifugation pellet (particulate organic matter and clay minerals) was discarded and the
152 brown surnatant sodium humate was reprecipitated with HCl and centrifuged. Finally the HA
153 in the gel state and acid pH was dialyzed in distilled water using cellophane bags (Visking®
154 dialysis tubing, molecular weight cutoff 12,000–14,000 Da; pore diameter *ca.* 25 Å,
155 Medicell) and desiccated at 40 °C.

156 *2.4. Characterization of the HA fraction*

157 The HAs were studied by pyrolysis-gas chromatography/mass spectrometry (Py-GC/MS),
158 and by visible and IR spectroscopies. The optical density, that is considered as a surrogate of
159 the aromaticity of HAs [25], was measured in solutions of 66.6 mg L^{-1} C in 0.02 mol L^{-1}
160 NaOH. Second-derivative spectra were acquired with a Shimadzu UV-240 OPI-2
161 spectrophotometer. The IR spectra of the HAs were obtained with a Shimadzu FTIR-8400 PC
162 using KBr dishes with 2.00 mg HA. In order to assist the visual inspection the broadband
163 profiles in the IR spectra from HAs, a resolution enhancement algorithm was applied based
164 in subtracting the raw spectrum (sized to 640 data points) from multiple (×60) of its second
165 derivative and further application of smoothing [26, 27].
166 Pyrolysis–gas chromatography–mass spectrometry (Py–GC/MS) was carried out using a
167 double-shot pyrolyzer device PY2020iD (Frontier Lab Ltd., Fukushima, Japan) attached to a
168 GC/MS system Agilent 6890 [28]. Samples of 1–2 mg in weight were pyrolyzed in small
169 crucible capsules introduced for 1 min into the micro-furnace preheated at 500 °C. The
170 evolved gasses were directly injected into the GC/MS for analysis. The GC was equipped
171 with a low-to-mid polarity fused silica capillary column DB-1701 (J&W Scientific) (30 m ×

250 μm × 0.25 μm film thickness), the oven temperature was held at 50 °C min^{-1}, and then increased up to 100 °C at 30 °C min^{-1}, from 100 to 300 °C at 10 °C min^{-1}, and stabilized at 300 °C for 10 min using a heating rate of 20 °C min^{-1}. The carrier gas used was helium at a flow of 1 mL min^{-1}. The detector was an Agilent 5973 mass selective detector and mass spectra were acquired with a 70 eV ionizing energy. Compound assignment was achieved *via* single-ion monitoring for various homologous series, *via* low-resolution mass spectrometry and comparison with published and stored data (NIST and Wiley libraries).

2.5. Statistical analyses

Data treatments were performed with the Statistica package [29]. The joint classification of soil and environmental variables in addition to variables corresponding to molecular characteristics of the SOM was carried out by a multidimensional scaling method [30].

3. Results

3.1. Spectroscopic characterization of the HAs

The HAs chosen for Py-GC/MS studies were selected through a previous exploratory analysis by visible (UV-Vis) and infrared (FT-IR) spectroscopy [19]. The results are summarized in Table 2 and Fig. 1 depicting the spectroscopic characteristics of two selected samples showing contrasting levels of residual lignin (i.e., high (19) and weak (16) lignin signature). The high lignin signature sample 19 displays IR conspicuous peaks at 1510, 1460, 1420, 1270, 1230 and 1030 cm^{-1}, just coinciding with a weak intensity of the peaks revealed in the second derivative (as valleys) in the visible spectrum at *ca.* 620, 570 and 530 cm^{-1}, typically interpreted as a biomarker feature of specific fungal metabolism [31]. The opposed situation is observed in sample 16, the HA with less marked lignin pattern and high optical density. Due to the suspected importance of the more or less defined lignin signature

observed in the resolution-enhanced FT-IR spectra, samples were ranked from high to low similarity to lignin and labelled with an ordinal (IR Lignin) used for data treatments as shown in Table 2.

3.1. Pyrolytic characterization of the HAs

Up to 250 different compounds could be detected in the pyrolysates of the studied samples and their relative yields with an indication of the possible precursor compounds [32] is shown in Table 3, where the relative abundance of the groups of compounds is coded with symbols indicating the levels of the semiquantitative percentages related to the total chromatographic area.

Methoxyphenols have been considered as an index for the persistence of plant-derived lignin in the less transformed structural domains of the HAs [33, 34]. Thus, accumulation of methoxyphenols would point to comparatively early humification processes with a weak structural alteration of macromolecular lignin, not necessarily requiring its complete breakdown into low molecular weight compounds.

When the HA samples are classified in terms of the more or less marked lignin pattern as seen in the IR spectra, it was possible to classify the samples in a gradient ranging between two extreme categories as previously illustrated in Fig. 1. The group of HAs showing 'weak lignin pattern' was characterized by major peaks of N-containing and carbohydrate-derived pyrolysis compounds, and poor yields of alkyl compounds (e.g., HA samples coded as M,N,O,P (samples #12, 4, 2, and 16), indicative of microbial metabolites accumulation and a more or less efficient biodegradation of plant-derived HA precursors. The major pyrolytic products in these samples consisted of non-methoxylated aromatic compounds (mainly alkylbenzenes), i.e., compounds that have been classically interpreted as typical pyrolytic proxies for matured HAs from terrestrial sources [35]. Despite the low potential of these

alkyl-substituted aromatic compounds as source indicator compounds, and to the fact that some might be derived from rearrangements of unsaturated aliphatic compounds during pyrolysis known to occur mainly in the presence of mineral catalysts [36], it is clear that both the stoichiometry of the pyrolysis compounds assemblages as well as the structure of the major fragments in this group of samples (Figs. 2 and 3) clearly diffrer from those expected from biomass constituents, as it would be the case for soil HAs for which C sequestration mechanisms could be assimilated to a selective preservation of plant and microbial constituents.

On the other side, the HA group showing a 'conspicuous lignin pattern' display a well-preserved methoxyphenol signature (i.e., guaiacol, syringol and their methyl-, ethyl-, vinyl-, propenyl- and acetyl- derivatives) and comparatively lower amounts of alkyl and N-derived pyrolysis products (HAs coded as A,B,C,D,E,F, corresponding to samples # 19, 10, 20, 9, 14 and 3).

Intermediate patterns between these two extreme situations were observed in HAs samples coded as G,H,I,J,K,L, corresponding to HAs # 11, 8, 6, 15, 17, 7, respectively illustrating the above-suggested simultaneous active humification processes contributing to SOM stabilization which also coincides with the occurrence of the mixed vegetation in these sites.

In some cases, the group of HAs with features pointing to a slow biodegradation of the original sources of SOM, *i.e.* the 'conspicuous lignin pattern', yielded aromatic pyrolysis products of relatively high molecular weight (e.g., biphenyls, compounds 149, 173, 126, 201) and well-defined, wide homologues series of alkanes, α,ω-alkanedienes and fatty acids. An outstanding systematic feature, particularly in HAs from soils developed under natural pine forest, was the release after pyrolysis of polyaromatic compounds (Fig. 2) such as phenanthrenes, retene and diterpene resin acids (e.g., dehydroabietic acid), which coincided with previous pyrolytic descriptors for pine soils in Mediterranen sites [4, 37].

The above differences between HA characteristics are in agreement with the previous exploratory analysis using only visible and IR spectroscopies, which also indicated a series of HAs with featureless IR spectra, high optical density (e.g., at 465 nm) and resolved peaks in the 2nd derivative visible spectra characteristic of polynuclear chromophors of fungal origin [31], which coincided with the 'weak lignin pattern' group of samples (Fig. 2). Another group of HAs presenting a comparatively marked aliphatic character and low molecular weight (intense 2920 cm^{-1} IR band, low optical density and IR spectra displaying typical lignin and amide bands), could be ascribed to group of samples with the 'conspicuous methoxyphenol pattern' betrayed by analytical pyrolysis.

4. Discussion

The results from Py-GC/MS suggested a variety of structural features in active biogeochemical scenarios which could be ordered as a gradient of progressive humification or SOM maturation [38]. This could be operatively interpreted as the results of a balance between non-excludent soil C sequestration processes, *i.e.* HAs with lignin domains at early alteration stages *vs.* HAs formed after heavy structural rearrangement of humic precursors not necessarily with a macromolecular nature.

In fact, in one extreme situation, soil HAs with spectroscopic and Py-GC/MS patterns indicative of heterogeneous composition suggest efficient microbial reworking of the SOM precursors, through humification mechanisms associating products from both plant or microbial synthesis, as well as secondary molecules and mixtures of oligomers released during litter biodegradation. The Ca^{2+}-saturated medium would favour the insolubilization of these humic precursors to be progressively arranged into supramacromolecular mixures. The broadband IR spectra of these HAs suggest few repeating structural units, and its high optical density is compatible with an advanced diagenetic 'maturation', i.e., selective biodegradation

of labile HA moieties and free-radical-induced cro ss-linking between components that are being randomly incorporated into the HA systems [3].

In other extreme situation, the characteristics of the HAs point to the preservation of comparatively young, lignoprotein-type substances, as betrayed by correlated spectroscopic and Py-GC/MS patterns suggesting that diagenetic stabilization of plant biomacromolecules and aliphatic structures are predominant C-sequestration mechanisms in the corresponding soils. Irrespectively to the more or less conspicuous lignin signature in the HAs, the sample groups did not significantly differ in terms of classical stoichiometric indices based on the yields of methoxyphenols (e.g., the classical syryngyl-to-guaiacyl ratio) which in many cases lead to accurately distinguish between land use or vegetation cover [39]. This is not unexpected in our case due to the large heterogeneity in terms of vegetation, soil use and HAs degree of maturity.

The above features are summarized in Fig. 4 where a variety of spectroscopic, pyrolytic and soil general characteristics with environmental relevance are classified by multidimensional scaling. This nonlinear mapping statistical procedure yields a reduced-dimensionality plot where the operative taxonomical units (in this case variables) are represented as points in the space defined by two dimensions calculated in a way in which the distances in the space are optimized to most closely fit the values of a similarity index (in this case the 1-Pearson correlation index) between the processed variables.

In this plot it is evident the association between the 'lignin signature in HAs' with the above indicated pyrolytic yields of methoxyphenols and aliphatic compounds, but also with soil physical and microtopographical features classically associated to moisture levels and accumulation of raw SOM (e.g., FOM). The other cluster of variables included characteristics typical of condensed, black-coloured HAs including fungal quinoid metabolites (E_{465}, Vis 620) in addition to non-methoxylated mono- or polycyclic pyrolysis

295 products. These HA characteristics appear correlated with physical and topographical factors
296 pointing to more conspicuous semiarid features in presumably flat, not intensely eroded areas
297 where clay accumulation and seasonal desiccation would presumably contribute to reach
298 advanced maturation of HAs. In fact, these soil-forming factors are classically described as
299 positive for the humification, *i.e.*, formation of recalcitrant HA-clay complexes and periodic
300 desiccation enhancing SOM insolubilization and condensation processes [14].

301 Additional statistical treatments mainly correspondence- and discriminant analyses (not
302 shown) failed in evidencing a substantial influence of vegetation types, soil use or direct
303 anthropogenic impact, a situation that has been previously described for similar calcimorphic
304 semiarid mountain ecosystems [12] and attributed to the homogeneizing or 'buffering'
305 physical and physiochemical effect of limestone (calcium saturation) on the different organic
306 matter forms (precipitation, encapsulation…). In a similar way, all unsupervised automated
307 classification of the HAs from our soils suggested that the continuous 'gradient' between
308 contrasting 'C-sequestration pathways' observed in our data, was quite independent as
309 regards to local features of soil use and vegetation and the major source of variability being
310 local-scale due to geomorphological factors [40] which are not currently recorded in most
311 studies on SOM dynamics, but that could play a relevant role in most calcium-saturated soils
312 where humification processes are not controlled by wide contrasts in soil reaction.

313

314 **5. Conclusions**

315 The analysis of the lignin-derived pyrolytic molecular assemblages in HAs suggests a
316 series of surrogate indicators of SOM quality based on the variable influence of soil C
317 stabilization mechanisms. This was the case with the relative yields of methoxyphenols
318 (which in this study paralleled the intensity of the lignin pattern in the IR spectra, and were
319 negatively related to the E_{465} optical density in the visible spectra) but also with the N-

containing, carbohydrate-derived and alkyl compounds. In general the above HA features could be useful for rapid discrimination of the prevailing humification processes influencing C-balance in calcimorphic soils . In this study, SOM quality (i.e., its most advanced stages of transformation) could be assimilated to the extent to which the HAs accumulated in the soil differ in its molecular composition as regards to the biomacromolecules from microbial and plant sources. For instance, the incorporation of specific biomarkers such as conifer resin constituents into the HA structure could represent a valid proxy for raw SOM preservation in forest ecosystems with comparatively low biogeochemical performance. On the opposite, conspicuous concentration of perylenequinone fungal chromophors in HAs (as seen in the 2^{nd} derivative visible spectra) would be pointing to the occurrence of intense microbial reworking of SOM leading to chaotic HA structures (broadband IR spectral profiles) and where the lignin spectroscopic signature is no longer evident by spectroscopic or pyrolytic approaches.

Acknowledgements

The authors wish to thank the Spanish Ministry of Science and Innovation by CTM2005-04739 / CGL2008-04926 / CARBORAR CGL2011-27493 / GEOFIRE CGL2012-38655-C04-01 research projects. Dr. Ana Piedra Buena has been contracted by the CCMA-CSIC via I3P Program supported by the European Social Fund. Dr. Isabel Miralles received postdoctoral fellowships Juan de la Cierva 2008-39669 and a Marie Curie Intra-European Fellowship (FP7-PEOPLE-2013-IEF, Proposal No. 623393)

References

[1] R. Lal, Soil carbon sequestration impacts on global climate change and food security, Science 304 (2004) 1623–1627.

[2] M. von Lützow, I. Kögel-Knabner, K. Ekschmitt, E. Matzner, G. Guggenberger, B. Marschner, H. Flessa, Stabilization of organic matter in temperate soils: Mechanisms and their relevance under different soil conditions—A review, Eur. J. Soil. Sci. 57 (2006) 426–445.

[3] G. Almendros, Humic substances, In: Ward Chesworth (ed) Kluwer Encyclopedia of Soil Science. Springer, Dordretch 2008, pp. 97–99.

[4] J. Schellekens, G.G. Barberá, P. Buurman, G. Pérez-Jordà, A. Martínez-Cortizas, Soil organic matter dynamics in Mediterranean A-horizons—The use of analytical pyrolysis to ascertain land-use history, J. Anal. Appl. Pyrol. 104 (2013) 287–298.

[5] F.J. Stevenson, Biochemistry of the formation of humic substances, In: Humus Chemistry, Wiley & Sons, Inc. New York 1982, pp. 195–220.

[6] M.H.B. Hayes, R.S. Swift, Genesis, isolation, composition and structures of soil humic substances. Soil Colloids and Their Associations in Aggregates, In: De Boodt MF, Hayes MHB and Herbillon A (eds) NATO ASI Series. Series B: Physics 215 (1990) 245–305.

368 [7] R. Sutton, G. Sposito, Molecular structure in soil humic substances: The new view,
369 Environ. Sci. Technol. 39 (2005) 9009–9015.
370
371 [8] A. Piccolo, The supramolecular structure of humic substances, Soil Sci. 166 (2001) 810–
372 832.
373
374 [9] A. Piccolo, The supramolecular structure of humic substances: A novel understanding of
375 humus chemistry and implications in soil science (Review), Adv. Agron. 75 (2002) 57–
376 134.
377
378 [10] G. Almendros, Z. Hernández, H. Knicker, J.A. González-Pérez, A. Piedra-Buena, F.J.
379 González-Vila, Humic substances as drivers of carbon flow and source of
380 biogeochemical proxies for climate change. MOLTER Conference 'SOM 2010', Organic
381 matter stabilization and ecosystem functions, p.67. Presqu'île de Giens (Côte d'Azur,
382 France) 19-23 September 2010. Available in the web at:
383 http://www.bioforsk.no/ikbViewer/Content/83713/Proceedings%20SOM2010%281%29
384 .pdf (Last consulted 27/010/2014)
385
386 [11] M.W. Schmidt, M.S. Torn, S. Abiven, T. Dittmar, G. Guggenberger, I.A. Janssens, M.
387 Kleber, I. Kögel-Knabner, J. Lehmann, D.A. Manning, P. Nannipieri, D.P. Rasse, S.
388 Weiner, S.E. Trumbore, Persistence of soil organic matter as an ecosystem property,
389 Nature. 478 (2011) 49–56.
390
391 [12] C. Oyonarte, A. Perez-Pujalte, G. Delgado, R. Delgado, G. Almendros, Factors
392 affecting soil organic matter turnover in a Mediterranean ecosystems from Sierra de

Gador (Spain): An analytical approach, Commun. Soil Sci. Plant. Anal. 25 (1994) 1929–1945.

[13] S. Derenne, K. Knicker, Chemical structure and preservation processes of organic matter in soils and sediments, Org. Geochem. 31 (2000) 607–608.

[14] P. Duchaufour, F. Jacquin, Comparaison des processus d'humification dans les principaux types d'humus forestiers, Bulletin Association Française pour l'Etude des Sols 1 (1975) 29–36.

[15] T.I. Stuczynski, G.W. McCarthy, J.B. Reeves, R.J. Wright, Use of pyrolysis GC/MS for assessing changes in soil organic matter quality, Soil. Sci. 162 (1997) 97–105.

[16] P.F. van Bergen, I.D. Bull, P.R. Poulton, R.P. Evershed, Organic geochemical studies of soils from the Rothamsted Classical Experiments—I. Total lipid extracts, solvent insoluble residues and humic acids from Broadbalk Wilderness, Org. Geochem. 26 (1997) 117–135.

[17] P. Buurman, P.F. van Bergen, A.G. Jongmans, E.L. Meijer, B. Duran, B. van Lagen, Spatial and temporal variation in podzol organic matter studied by pyrolysis-gas chromatography/mass spectrometry and micromorphology, Eur. J. Soil. Sci. 56 (2005) 253–270.

[18] S. Rivas Martínez. Memoria del Mapa de Series de Vegetación de España 1:400.000. ICONA, Madrid, 1987.

[19] I. Miralles, R. Ortega, M. Sánchez-Marañón, M. Soriano, G. Almendros, Assessment of biogeochemical trends in soil organic matter sequestration in Mediterranean calciimorphic mountain soils (Almería, Southern Spain), 324 Soil Biol. Biochem. 39 (2007) 2459–2470.

[20] CSIC, Métodos Analíticos de la Estación Experimental del Zaidín. CSIC, Granada 1969, Spain.

[21] L.A. Richards, Diagnosis and Improvement of Saline and Alkaline Soils, United States Salinity Laboratory Staff. Agricultural Handbook No 60. United States Department of Agriculture 1954, 160 p.

[22] D.V. Nelson, L.E. Sommers, Total carbon, organic carbon and organic matter, In: Page AL, Miller RH, Keeney DR (eds) Methods of Soil Analysis: Part 2, Chemical and Microbiological Properties, 2nd ed. American Society of Agronomy, Madison 1982, WI, pp. 539–579.

[23] M.E. Sumner, W.P. Miller, Cation exchange capacity and exchange coefficients, In: Sparks D.L. (ed) Methods of Soil Analysis, Part 3. Chemical Methods. Soil Science Society of America 1996, Book series No. 5.

[24] B. Dabin, Etude d'une méthode d'extraction de la matière humique du sol, Science du Sol 1 (1971) 47–63.

443 [25] S.J. Traina, J. Novak, N.E. Smeck, An ultraviolet absorbance method of estimating the
444 percent aromatic carbon content of humic acids, J. Environ. Qual. 19 (1990) 151–153.
445
446 [26] A. Rosenfeld, A.C. Kak, Digital Picture Processing, vol 1. 2nd ed. Academic Press, NY
447 1982.
448
449 [27] G. Almendros, J. Sanz, A structural study of alkyl polymers in soil after perborate
450 degradation of humin, Geoderma 53 (1992) 79–95.
451
452 [28] C.P. Assis, J.A. González-Pérez, J.M. de la Rosa, I. Jucksch, E.D. Mendonça, F.J.
453 González- Vila, Analytical pyrolysis of humic substances from a Latosol (Typic
454 Hapludox) under different land uses in Minas Gerais, Brazil, J. Anal. Appl. Pyr. 93
455 (2012) 120–128.
456
457 [29] StatSoft Inc., STATISTICA Data Analysis Software System, version 7.1. (2005)
458 www.statsoft.com
459
460 [30] J.B. Kruskal, Multidimensional scaling by optimising goodness of fit to a nonmetric
461 hypothesis, Psichometrika 29 (1964) 1–27.
462
463 [31] K. Kumada, H.M. Hurst, Green humic acid and its possible origin as a fungal
464 metabolite, Nature 214 (1967) 631–633.
465
466 [32] D.F.W. Naafs. What are humic substances? A molecular approach to the study of
467 organic matter in acid soils. PhD Thesis. Universiteit Utrecht, 2004.

[33] F. Martín, C. Saíz-Jiménez, F.J. González-Vila, Pyrolysis-gas chromatography-mass spectrometry of lignins, Holzforschung 33 (1979) 210–212.

[34] P. Tinoco, G. Almendros, F.J. González-Vila, Impact of the vegetation on the lignin pyrolytic signature of soil humic acids from Mediterranean soils, J. Anal. Appl. Pyrol. 64 (2002) 407–420.

[35] H.R. Schulten, M. Schnitzer, A state of the art structural concept for humic substances, Naturwissenschaften. 80 (1993) 29–30.

[36] C. Saíz-Jiménez, Analytical pyrolysis of humic substances: Pitfalls, limitations, and possible solutions. Environ. Sci. Technol. 28 (1994) 1773–1780.

[37] N.T. Jiménez-Morillo, J.A. González-Pérez, A. Jordán, L.M. Zavala, J.M. de la Rosa, M. Jiménez-González, F.J. González-Vila. Organic matter fractions controlling soil water repellency in sandy soils from the Doñana National Park (SW Spain). Land Degrad. Dev. DOI: 10.1002/ldr.2314 (First published online: 5 AUG 2014).

[38] I. Miralles, R. Ortega, G. Almendros, M. Sánchez-Marañón, M. Soriano, Soil quality and organic carbon ratios in mountain agroecosystems of South-East Spain, Geoderma 150 (2009) 120–128.

[39] C.N. Jex, G.H. Pate, A.J. Blyth, R.G.M. Spencer, P.J. Hernes, S.J. Khan, A. Baker, Lignin biogeochemistry: from modern processes to Quaternary Archives. Quaternary Sci. Rev. 87 (2014) 46–59.

[40] A. Piedra-Buena, I. Miralles, R. Ortega, Z. Hernández, G. Almendros, Molecular proxies responsive to the effect of microtopographical constraints on soil C sequestration processes in mountain Mediterranean ecosystems (Almería, Spain). Soil Geography: New Horizons. 16-20 Noviembre. Huatulco, Santa Cruz, Oaxaca, México (2009).

505 **FIGURE CAPTIONS**

506 Fig. 1. Spectroscopic patterns of humic acids from semiarid calcimorphic soils representative
507 of extreme levels of residual lignin (left: sample 19 with high lignin signature; right sample
508 16 with low lignin signature). Top: IR spectra in the 2000–700 cm^{-1} range, superimposed to
509 the corresponding resolution-enhanced IR spectra. Below: visible spectra and their 2nd
510 derivatives.

511

512 Fig. 2. Relative amounts of different group of pyrolysis products in humic acids from
513 semiarid mountain calcimorphic soils, classified by lignin pattern group as originally defined
514 by the intensity of the lignin pattern in the IR resolution-enhanced IR spectra (Fig. 1).

515

516 Fig. 3. Average values and confidence limits of relative amounts of the pyrolysis products in
517 humic acids from semiarid mountain calcimorphic soils classified by compound group.

518

519 Fig. 4. Automatic classification by multidimensional scaling (final stress = 0.175) of
520 variables corresponding to HA characteristics (solid circles) together with soil analytical
521 properties and environmental factors with a bearing on the humification process (void
522 circles), using the 1-Pearson index as similarity criterion. The plot shows two extreme
523 situations of variable characteristics: a) humic acids presumably derived from diagenetic
524 transformation of lignins preserved in soil; b) variables associated to HAs in advanced
525 transformation stages where lignin signature is not evident. Variables in the middle of the
526 scatterdiagram show no strong trends as regards transformation of lignin in the studied soils.
527 Variables obtained with a Geographical Information System: GSR_E: global solar radiation
528 at equinox; GSR_S: global solar radiation at summer solstice; GSR_W: global solar radiation

529 at winter solstice; HS_E: hours of insolation at equinox; HS_S: hours of insolation at
530 summer solstice; HS_W: hours of insolation at winter solstice; LSF: length slope factor; R:
531 contributing area; SPlanC: slope plan curvature; SProfileC: slope profile curvature; W:
532 wetness index.

533 Soil physical and chemical variables and humic acid characteristics (solid circles):

534 C: Total soil C; E_{465}: optical density of the HA at 465 nm; FOM: concentration of free
535 organic matter; HA: concentration of soil humic acid; IR Lignin: intensity of the lignin
536 pattern in the IR spectra; Sand, Clay: granulometric fractions; Tot Por: Total porosity; Vis
537 620: absorption at 620 nm in the 2^{nd} derivative visible spectrum.

538 Total abundances of the main groups of pyrolysis compounds are shown with their formulas

539

540

541 **Table 1** General characteristics of soils in mountain calcimorphic semiarid ecosystems

Sample/ code[a]	Soil type	Vegetation[b]	Geological substrate	Total sand (2–0.02 mm) g kg^{-1}	Total clay (<0.002 mm) g kg^{-1}	WHC g cm^{-3}	pH (H_2O)	$CaCO_3$ g kg^{-1}	Soil C g kg^{-1}	C/N	CEC $cmol_c$ kg^{-1}
2 / O	Rendzic Leptosol	Brush encroached	Clastic limestone	391	237	140	8.3	528	18.6	11.5	21.5
3 / F	Hypocalcic Calcisol	Relictual oak	Detritic limestones and marls	327	397	283	7.7	278	81.2	18.8	41.9
4 / N	Hypercalcic Calcisol	Reforested pine	Detritic limestones	597	189	117	8.0	673	31.3	13.9	25.0
6 / I	Hypercalcic Calcisol	Climacic pine	Clastic limestones	414	292	193	8.2	313	32.2	16.1	30.7
7 / L	Hypercalcic Petric Calcisol	Cereal	Detritic sediments	572	173	118	8.5	588	13.2	12.4	12.7
8 / H	Petric Calcisol	Reafforested pine forest (Pinus halepensis)	Marls and limestones	513	108	59	8.4	940	13.2	16.0	9.2
9 / D	Calcic Chernozem	Climacic pine	Detritic limestones	257	272	341	7.9	360	85.4	29.8	53.9
10 / B	Calcic Chernozem	Climacic pine	Detritic limestones and dolomies	344	324	267	8.1	544	74.4	37.7	7.9
11 / G	Calcaric Rendzic Leptosol	Alpine brush	Limestones	110	490	412	7.7	46	107.4	10.3	50.4
12 / M	Gleyc Hypocalcic Calcisol	Orchard	Alluvial calcic marls	69	668	209	8.3	439	6.9	8.1	24.8
14 / E	Mollic Calcaric Cambsiol	Relictual oak	Limestones	74	554	252	7.6	5	50.3	14.3	37.6
15 / J	Hypercalcic Petric Calcisol	Chaparral-like brushland	Limestones	161	475	290	8.0	294	49.0	13.5	35.9
16 / P	Calcaric Rendzic Leptosol	Chaparral-like brushland	Limestones	64	516	325	7.9	42	52.9	8.0	37.1
17 / K	Hypercalcic Calcisol	Cereal	Limestones	331	293	161	8.2	674	23.4	9.7	17.1
19 / A	Mollic Calcaric Cambisol	Climacic pine	Detritic limestone material	508	309	521	7.3	248	195.3	15.1	46.2
20 / C	Calcaric Rendíc Leptosol	Alpine brush	Limestones	203	482	238	7.9	380	25.0	3.9	26.9

542 [a] One-character code used in Table 3 to refer the contribution of lignin in the HA structure

543 [b] Reforested pine: *Pinus halepensis*; Bush encroached cleared site: *Stipa tenacissima, Lygeum spartum, Genista scorpius, Artemisia* sp.; Relictual oak:
544 *Quercus ilex* ssp. *rotundifolia*; Orchard: almond trees; Climatic pine: *Pinus halepensis*; Climacic pine: *Pinus nigra* (9, 10), *Pinus halepensis* (19); Alpine
545 brush: *Juniperus oxycedrus, Vella spinosa, Erinacea antillis, Quercus coccifera* (11), *Vella spinosa, Erinacea antillis, Lygeum spartum* (20); Chaparral-like
546 brushlands: *Quercus ilex* ssp. *rotundifolia, Juniperus phoenicia*. WHC: water holding capacity; CEC: cation exchange capacity.

Table 2 Soil organic matter characteristics and spectroscopic properties of humic acids from mountain calcimorphic semiarid soils

Sample/ code[a]	FOM (C g 100 g soil^{-1})	HA (C g 100 g soil^{-1})	E_{465}	E 620	IR Lignin
2 / O	1.2	21.3	1.23	0.0024	5
3 / F	2.9	25.5	0.56	0.0016	14
4 / N	0.6	54.3	0.66	0.0018	3
6 / I	2.0	57.7	0.71	0.0019	13
7 / L	2.5	52.0	0.97	0.0018	12
8 / H	2.4	51.9	0.63	0.0021	11
9 / D	1.6	10.0	0.86	0.0020	10
10 / B	1.0	10.5	0.73	0.0019	9
11 / G	6.5	89.7	0.84	0.0020	6
12 / M	0.9	63.2	1.26	0.0020	2
14 / E	4.3	23.8	0.62	0.0009	8
15 / J	4.3	12.2	0.95	0.0021	4
16 / P	1.4	2.7	1.10	0.0019	1
17 / K	1.5	37.6	0.87	0.0021	7
19 / A	4.0	13.5	0.52	0.0015	15
20 / C	2.5	7.4	0.64	0.0028	16

[a] One-character code used in Table 3 to refer the contribution of lignin in the HA structure.
FOM: Free organic matter, HA: Humic acid; E_{465}: Optical density values at 625 nm in the visible range in absorption units; E 620: Intensity of the valley at 620 nm in the second derivative spectrum in absorption units; IR Lignin: relative intensity of the lignin pattern in the IR spectra.

Table 3 Pyrolysis products identified in different groups of humic acids[a] with an indication of their relative yields and possible precursor (in brackets)

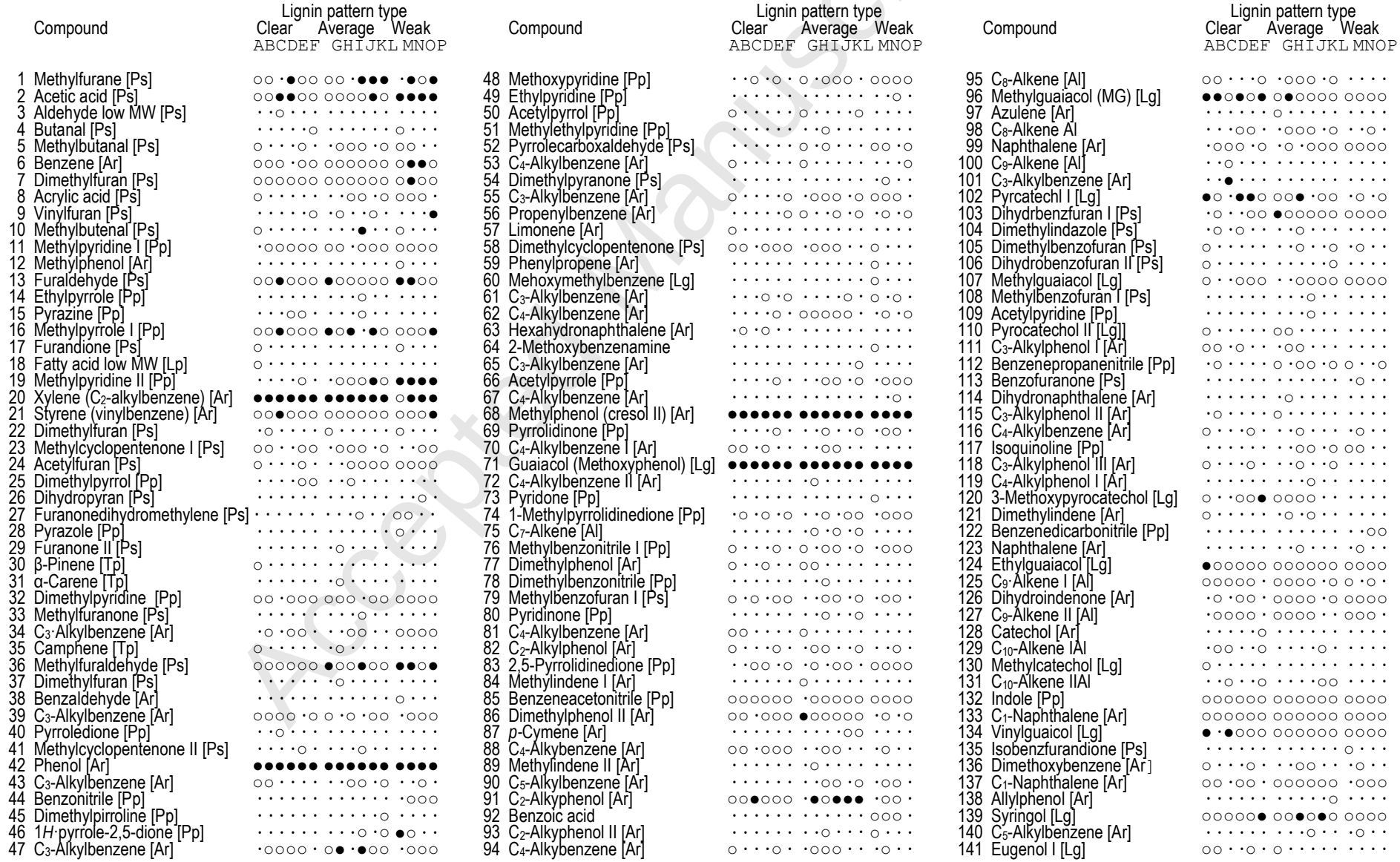

	Compound	Lignin pattern type: Clear ABCDEF	Average GHIJKL	Weak MNOP
142	Propylguaiacol [Lg]	○··○○·····	·····	····
143	C_{11}-Alkene [Al]	○·····	·····	····
144	Benzonitrile [Pp]	·····	·····	··○·
145	Hydroxybenzonitrile [Pp]	····○·	···○··	·○·○
146	Trimethylindene [Ar]	○·····	·····	····
147	Ethylcatechol [Lg]	○·····	·····	····
148	C_{11}-Alkene IAl	·····	···○··	····
149	Biphenyl [Ar]	···○○·	○·○○·	○○○○
150	Methylindole [Pp]	○○·○○○	○○○○○○	○○○○
151	Vanillin [Lg]	○·○···	·····	○○··
152	C_{11}-Alkene II [Al]	··○···	·····	○···
153	C_{11}-Fatty acid [Lp]	·····	····○·	····
154	Alkene C_{11} [Al]	·○○○·	·····	····
155	Methylbenzofurandione [Ps]	·····	·○····	····
156	Eugenol II [Lg]	○···○·	·····	····
157	C_2-Naphthalene [Ar]	··○·○○	○○○○○·	·○○○
158	Trimethylbenzaldehyde I [Ps]	○·····	··○○·○	····
159	C_2-Naphthalene [Ar]	○○··○·	·○○○○○	·○··
160	Methylsyringol [Lg]	·○○○○○	·○○·○·	·○··
161	Eugenol III [Lg]	·····	··○···	····
162	C_4-Phenol II [Ar]	·····	○·····	····
163	Hydroxyphenylethanone [Ar]	·····	···○··	··○·
164	Propenylguaiacol [Lg]	○○○·	○○·○○○	··○·
165	Coumaric acid [Ps]	·····	·····	·○··
166	C_2-Naphthalene III [Ar]	○··○··	·○·○··	·○··
167	Phenylpyridine [Pp]	·····	○·····	··○·
168	Isoindole [Pp]	·····	○····	○···
169	Isoindoledione [Pp]	·○○○○·	○·○○·	○○·○
170	Acetoguaiacone [Lg]	○○○○●●	○○○○●	○○○○○
171	C_{12}-Alkene I [Al]	○○·····	·····	····
172	C_{12}-Alkene II [Al]	○○○○○○	○○○○·	○○··
173	Methylbipheny [Ar]	·····	·····	·○○·
174	Dimethylindoledione [Pp]	·····	··○○·	○·○·
175	Ethylsyringol [Lg]	··○··	○○○·	○○··
176	Guaiacylacetone I [Ps]	○···○○	···○○○	·○··
177	Dibenzofuran [Pp]	·····	·····	·○○○
178	C_3-Naphthalene I [Ar]	○··○○·	·○····	○···
179	C_3-Naphthalene II [Ar]	○·····	·····	····
180	Isocyanonaphthalene [Ar]	·····	·····	··○·
181	C_{12}-Fatty acid [Lp]	○··○○·	·····	··○·
182	Hydroxyquinolinone [Pp]	·····	··○··	○···
183	Vanillic acid [Ar]	○···○·	·○···	○···
184	Vinylsyringol [Lg]	··○···	·○○·○○	·○○·
185	C_3-Naphthalene III [Ar]	·○○○·	○○○○○	·○○·
186	C_{13}-Alkene [Al]	··○○··	○···○	··○·
187	Isoquinoledione [Pp]	····○·	·○○○·	○·○○
188	C_3-Naphthalene IV [Ar]	·●○·○·	○○○○○○	·○··
189	Fluorene [Ar]	·····	·····	··○·
190	C_{13}-Alkene I [Al]	····○·	···○··	····
191	C_{13}-Alkene II [Al]	○·○○○○	○○·○··	····
192	C_3-Naphthalene V [Ar]	●····○	·····	····
193	Methoxyeugenol [Lg]	·····	○·····	····
194	Phenylbenzenamine [Pp]	····○○	··○···	○○··
195	C_{13}-Fatty acid [Lp]	○·····	·····	····
196	Methylnaphthalenol	○·····	·····	····
197	Phenoxyphenol [Lg]	·····	·····	·○··
198	Methoxydimethylindole [Pp]	·····	·····	○···
199	C_{10}-Alkybenzene [Ar]	·····	·····	○···
200	Propenylsyringol [Lg]	··○·○○	··○·○○	····
201	Dimethylbiphenyl [Ar]	○·····	·····	····
202	C_{14}-Alkene I [Al]	○○○○○·	·○··○○	··○·
203	C_{14}-Alkene II [Al]	○·○···	··○·○○	○·○·
204	Camazulene I [Ar]	○·····	·····	····
205	C_{14}-Alkene III [Al]	○·····	·····	····
206	Acetylsyringol [Lg]	○·····	··○···	····
207	Camazulene II [Ar]	·○·○·○	·○·○··	··○·
208	$C_{14:1}$-Fatty acid [Lp]	○·····	·····	····
209	C_{14}-Fatty acid [Lp]	●●○●○●	○○○○○○	·○○○
210	Acetylsyringol [Lg]	··○·○○	○···○○	·○··
211	C_{15}-Alkene I [Al]	○○○○··	○○·○○·	····
212	C_{15}-Alkene II [Al]	○○○○○·	○○··○○	○···
213	Phenanthrene [Tp]	·····	···○···	·○○·
214	C_{15} *iso*-Fatty acid [Lp]	○○·○○·	○○···○	○···
215	C_{15} *anteiso*-Fatty acid [Lp]	○○·○○·	○○··○○	····
216	Syringic acid	·····○	····○·	····
217	C_{15}-Fatty acid [Lp]	○○○○○○	○○··○○	····
218	Dimethoxyphenol [Ar]	·····	○·····	····
219	C_{15}-Alkylnitrile [Pp]	·····	··○·○○	○·○·
220	C_{16}-Alkene I [Al]	○··○··	○○··○●	····
221	Methylphenanthrene I [Tp]	○○·○··	···○···	·○○·
222	C_{16}-Alkene II [Al]	··○○··	··○○○·	·○··
223	$C_{16:1}$-Fatty acid [Lp]	·○···○	·····○	····
224	C_{16}-Fatty acid [Lp]	●●○●●●	●●○○●●	○○○○
225	C_{17} *iso*-Fatty acid [Lp]	○·····	·····	····
226	C_2-Phenantrene [Tp]	○○·○○·	·○○○··	·○·○
227	C_{17} *anteiso*-Fatty acid [Lp]	·····	·····○	····
228	C_{17}-Alkene [Al]	·●····	·····○	····
229	C_{17}-Fatty acid [Lp]	·○···○	○·····	····
230	Octadecanenitrile [Pp]	·····	·····○	····
231	Hexadecanamide [Pp]	·○····	·····	····
232	Dimethoxyphenanthrene [Tp]	○·····	·····	····
233	C_{18}-Alkene [Lp]	○··○○○	○·○·○○	····
234	$C_{18:1}$-Fatty acid [Lp]	·····	○·····	····
235	C_{18}-Fatty acid [Lp]	···○○●	·○○○○○	····
236	Trimethylphenanthrene [Tp]	○○·○○·	···○··	····
237	Retene [Ar]	●○····	·○○○··	·○··
238	Dehydroabietane [Tp]	○○·○··	·····	····
239	Dehydroabietic acid [Tp]	●○·○··	·○····	····
240	Abietic acid [Tp]	○·····	·····	····

[a] Sample sets: Lignin pattern, based in the observation of the IR spectra: "Clear"= ABCDEF: 19, 10, 20, 9, 14, 3, respectively; 'Average' = GHIJKL: 11, 8, 6, 15, 17, 7 respectively; 'weak' = MNOP: 12, 4, 2, 16, respectively (Figure 2).

Total abundance referred to total volatile compounds: · = 0 %; ○ = 0–2 %; ● = >2 %.

Origin: Lg: lignin; Ps: carbohydrate; Lp: lipid; Ar: unspecific aromatic (methoxyl-lacking); Pp: peptides; Tp: terpenoid. Roman numbers indicate different isomers.

Figure 1

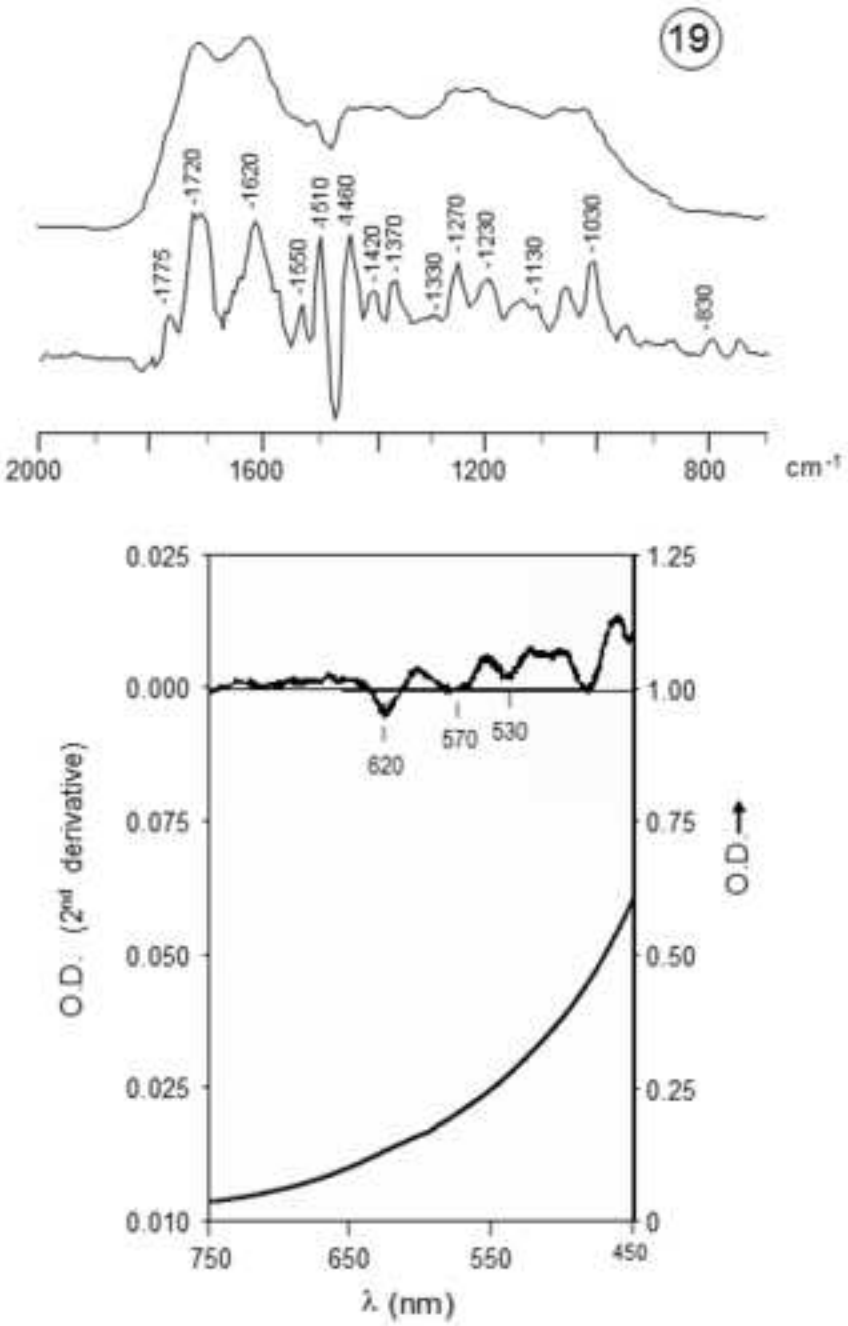
19
1775
1720
1620
1550
1510
1460
1420
1370
1330
1270
1230
1130
1030
830
2000
1600
1200
800
cm-1
0.025
0.000
0.075
0.050
0.025
0.010
1.25
1.00
0.75
0.50
0.25
0
620
570
530
750
650
550
450
λ (nm)
O.D. (2nd derivative)
O.D.

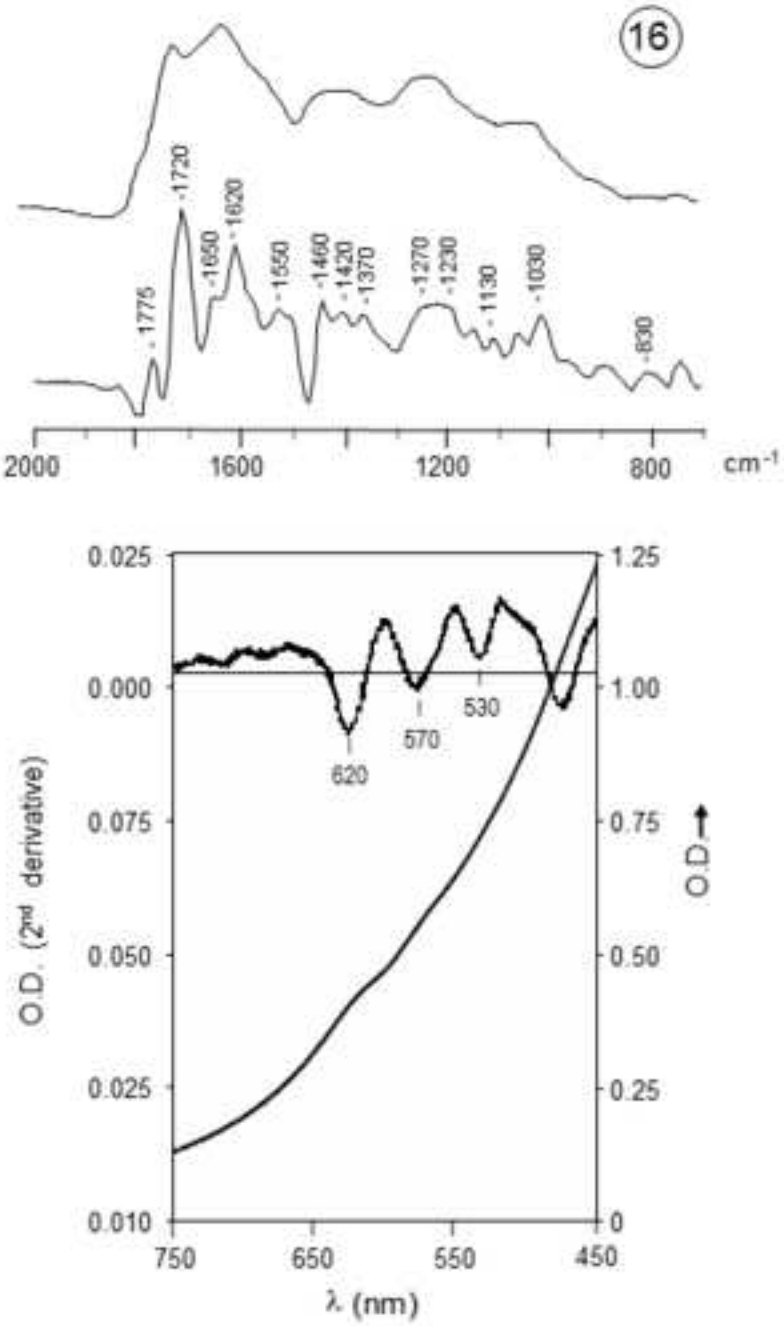
16
1775
1720
1650
1620
1550
1460
1420
1370
1270
1230
1130
1030
830
2000
1600
1200
800
cm-1
0.025
0.000
0.075
0.050
0.025
0.010
1.25
1.00
0.75
0.50
0.25
0
620
570
530
750
650
550
450
λ (nm)
O.D. (2nd derivative)
O.D.

Figure 2

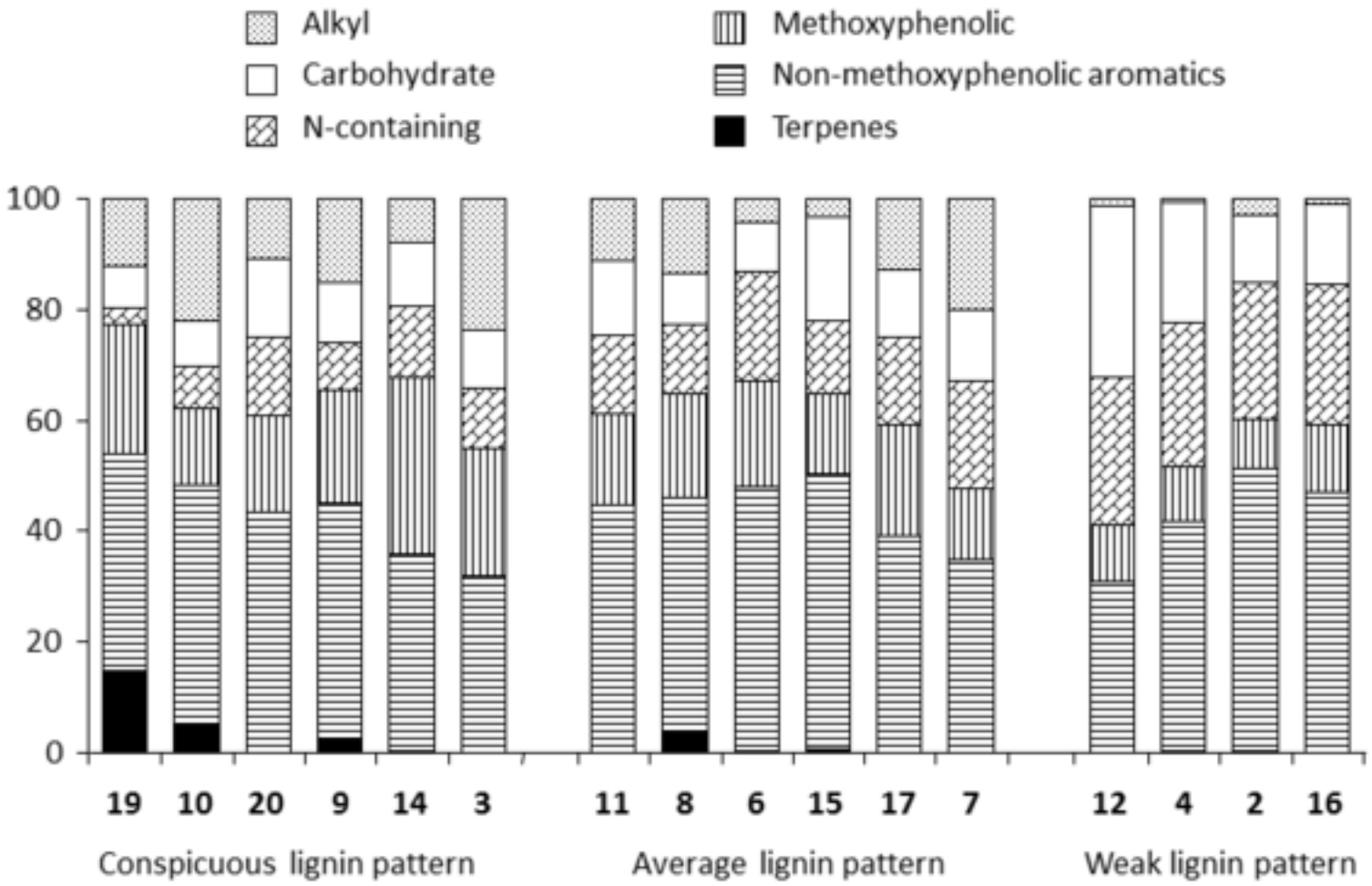
Alkyl
Carbohydrate
N-containing
Methoxyphenolic
Non-methoxyphenolic aromatics
Terpenes
100
80
60
40
20
0
19 10 20 9 14 3
11 8 6 15 17 7
12 4 2 16
Conspicuous lignin pattern
Average lignin pattern
Weak lignin pattern

Figure 3

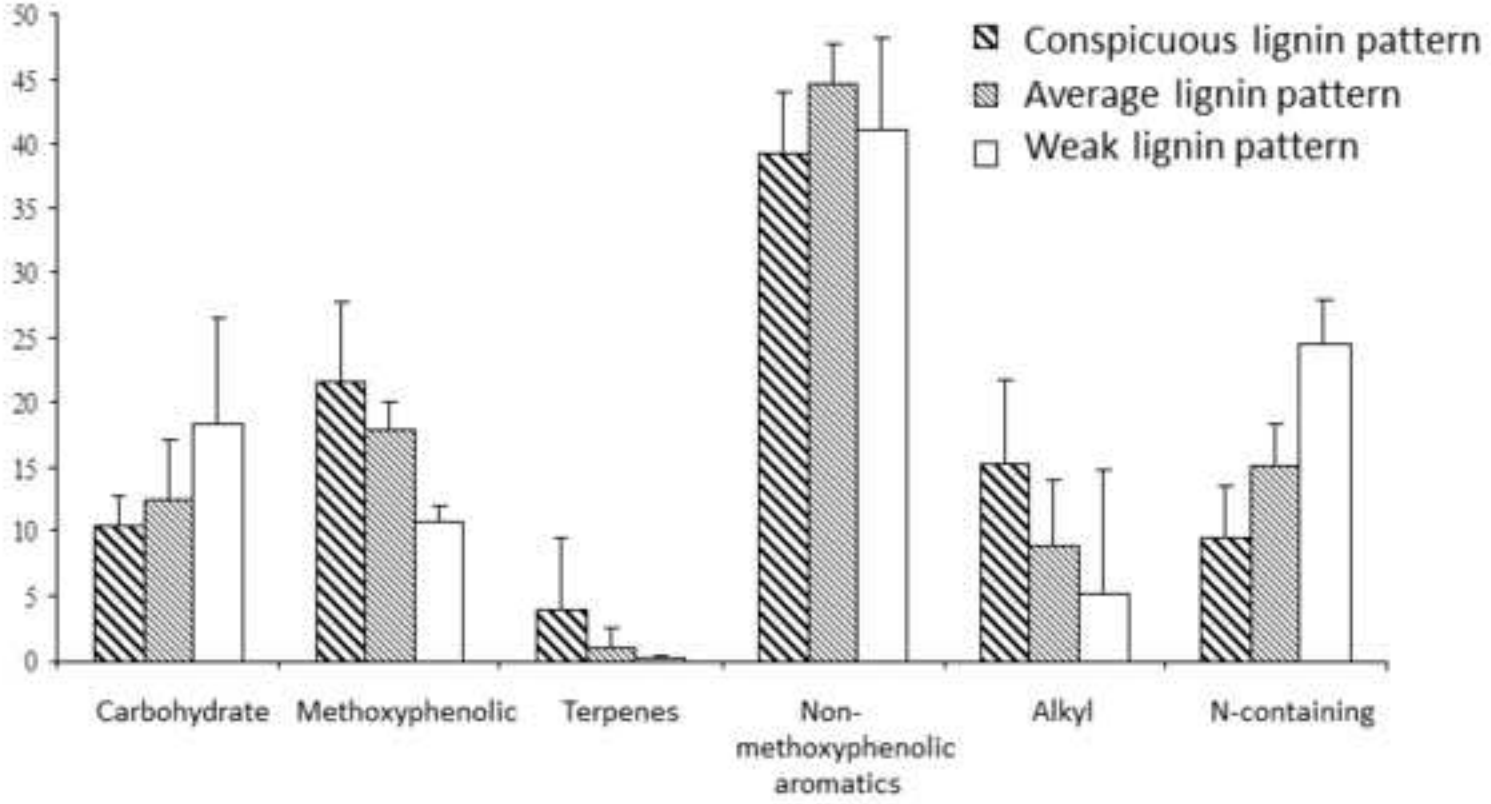
50
45
40
35
30
25
20
15
10
5
0
Conspicuous lignin pattern
Average lignin pattern
Weak lignin pattern
Carbohydrate
Methoxyphenolic
Terpenes
Non-methoxyphenolic aromatics
Alkyl
N-containing

Figure 4

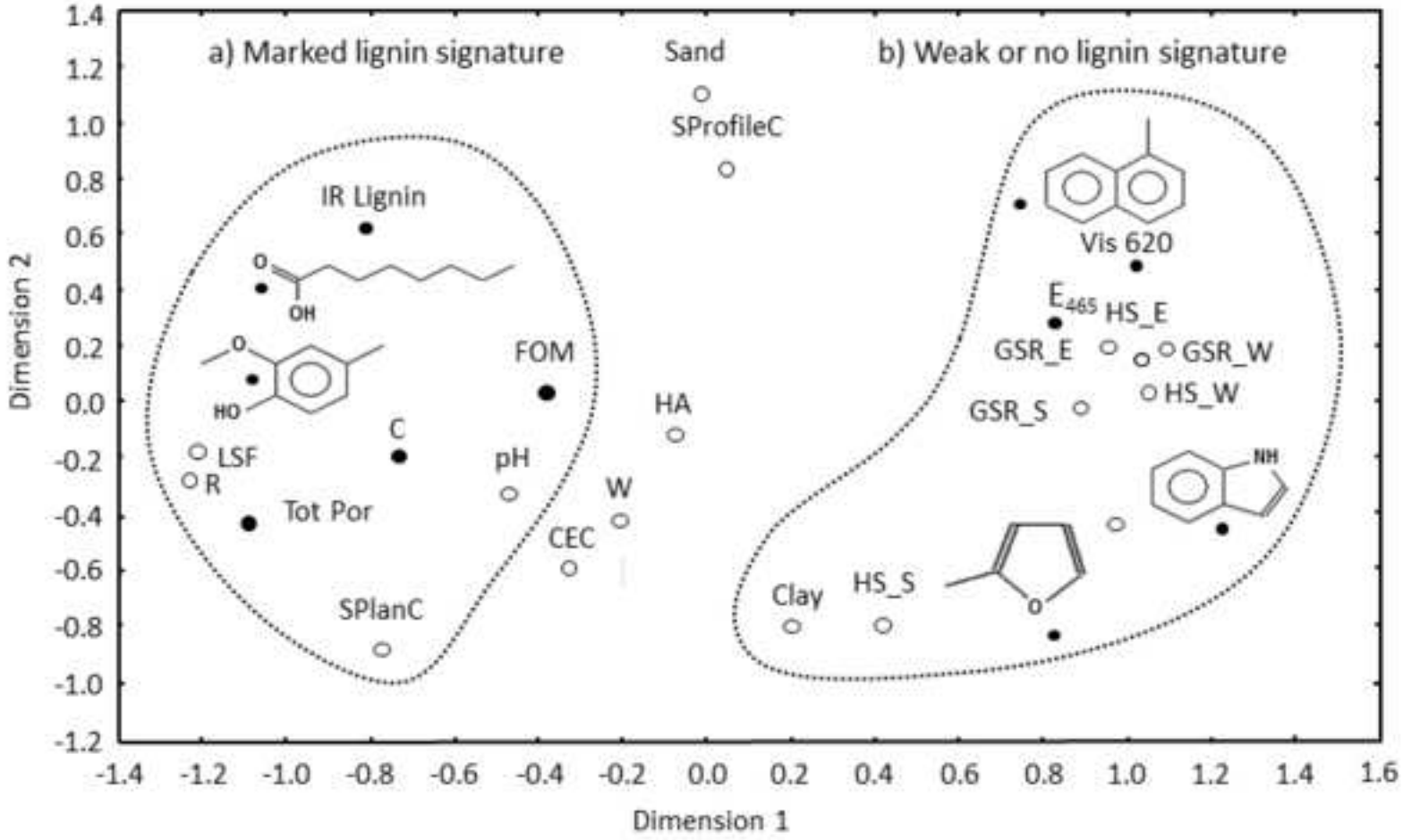
a) Marked lignin signature
b) Weak or no lignin signature
Sand
SProfileC
IR Lignin
Vis 620
E_{465}
HS_E
GSR_E
GSR_W
HS_W
GSR_S
FOM
HA
C
LSF
R
Tot Por
pH
W
CEC
SPlanC
Clay
HS_S
OH
HO
NH
Dimension 1
Dimension 2
1.4
1.2
1.0
0.8
0.6
0.4
0.2
0.0
-0.2
-0.4
-0.6
-0.8
-1.0
-1.2
-1.4
-1.2
-1.0
-0.8
-0.6
-0.4
-0.2
0.0
0.2
0.4
0.6
0.8
1.0
1.2
1.4
1.6

Highlights

Humic acids were studied by UV/VIS, FT–IR and Py-GC/MS

Pyrolytically-released methoxyphenols paralleled spectroscopic markers of lignin

Lignin signature in humic acids as an index for soil carbon stabilization